Magnetic properties of superconducting K_3C_{60} and Rb_3C_{60} synthesized from large single-crystal fullerenes

S. H. Irons, J. Z. Liu, P. Klavins, and R. N. Shelton
Department of Physics, University of California at Davis, Davis, California 95616
(Received 10 July 1995)

Single crystals of C_{60} were doped with alkali metal (K and Rb), characterized, and measured magnetically in fields up to 5 T. Detailed experiments show the samples to be of high quality with superconducting transition widths on the order of 1 K. Data on the field and temperature dependences of the critical current density J_C and H_{C1} are presented. We find that while the general behavior is similar to that of powder specimens, there are significant differences when comparing magnitudes. We attribute these differences to the fact that powder samples have much more surface area per volume than single crystals which can affect the determination of superconducting parameters. The critical current density also shows clear differences when compared to polycrystalline samples. In addition, comparisons between K_3C_{60} and Rb_3C_{60} indicate that defects may be more prevalent in the latter compound due to more sensitive synthesis requirements.

INTRODUCTION

Since the discovery of superconductivity in alkali-doped C_{60} systems,[1,2] there has been a concentrated effort to determine the intrinsic properties of these compounds. These materials present a challenge, not only from the standpoint of sample preparation, but analysis as well. This difficulty is due to several factors. Most notably, the process through which the samples are synthesized requires the controlled intercalation of alkali metals. In addition, to properly analyze results, questions of sample homogeneity must be addressed. The air sensitivity of alkali metals provides a further hardship when performing measurements. As a result, the vast majority of the early data collected on the superconducting properties of these compounds has been collected using powder samples.[3–5] The use of polycrystalline powders allows samples to be made in sufficiently large quantities to stoichiometrically control the amount of intercalant and also to achieve a high sample homogeneity. However, in powders, intergrain effects and the large surface area often cause a broadening of T_c, which can lead to large errors in the measurement of other intrinsic properties.

By using single crystals, these problems associated with powders can be avoided. However, when single crystals first became available, they were too small to dope stoichiometrically. For this reason transport measurements were used to control the doping and simultaneously investigate properties.[6,7] While transport allows one to directly monitor the doping process, it is not always the case that bulk properties are being investigated. By probing the single crystals magnetically, a bulk measurement can be obtained. Yet, to achieve optimal doping, the process must be done stoichiometrically since leads cannot be attached without affecting the measurement. This requires large samples ($\sim$1 mg or greater) in order to adequately control the amount of alkali metal introduced into the vacant octahedral and tetrahedral sites of the C_{60} lattice. A clear disadvantage is that one cannot directly monitor the doping process. Still, by using a consistent method, this difficulty can be overcome.

We report results obtained using a superconducting quantum interference device (SQUID) magnetometer[8] on large crystals of C_{60} doped with potassium and rubidium, in fields up to 5 T and temperatures down to 5 K. These data are used to obtain quantitative estimates of $H_{c1}(0)$ and J_c. Analysis indicates significant differences from existing reports of magnetic measurements on powders. In addition, we provide the temperature and field dependences for the critical current density.

SAMPLE SYNTHESIS AND CHARACTERIZATION

C_{60} powder was synthesized by vaporizing graphite rods in a helium arc furnace,[9] and then separated and purified via a standard chromatographic technique.[10] Before use, the powder was vacuum dried to remove residual solvents. Crystals were grown using a modified version of a vacuum sublimation process detailed in the literature.[11] Between 5 and 15 mg of C_{60} powder were pelletized and placed in a gold boat inside an 8-mm-i.d. quartz tube. After being heated under vacuum ($\sim 10^{-6}$ Torr) overnight at 275 °C to remove any remaining solvent and water vapor, the quartz tube was sealed. Crystal growth was carried out in a double gradient furnace with a typical temperature profile shown in Fig. 1.

Growth times ranged from 1 to 4 days with crystals sizes ranging from 0.5 to 10 mg. While varying parameters such as the growth zone size, source and growth region temperatures, and growth time induced modest changes in the crystal output and morphology, by far the most dramatic effects were observed when the source material was changed. If this material is highly crystalline with nearly macroscopic grain sizes, the growth rate will be high and the number of nucleation sites limited to 1 or 2. With fine powder as a starting material, many more crystals nucleate leading to smaller average sizes. In this instance, there is also a greater incidence of a reddish dusty patina covering some of the crystals. We suspect that this surface discoloration is due to ultrafine C_{60} powder that has been adsorbed onto the surface of the crystal as a thin film. This method allows for rapid synthesis ($\sim$2–3 days) of large, high-quality crystals with only a small amount

0163-1829/95/52(21)/15517(5)/$06.00

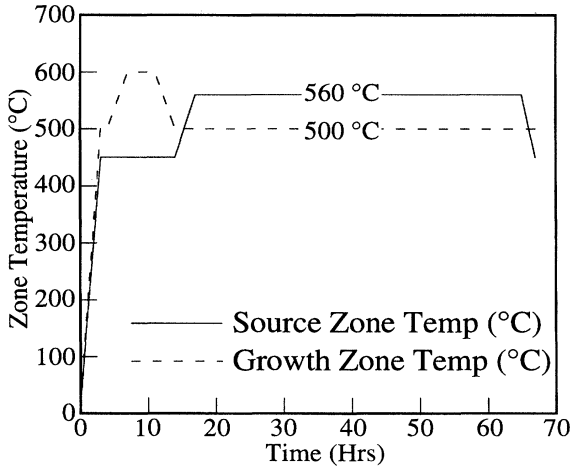

FIG. 1. Furnace temperature profile for C_{60} crystal growth.

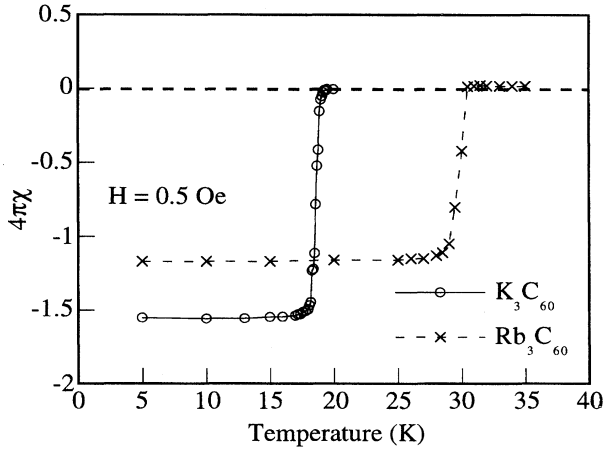

FIG. 2. Zero-field-cooled (ZFC) curves for $4\pi\chi$ vs T for K_3C_{60} and Rb_3C_{60}. $T_c = 19.3$ and 30 K defined by onset.

of starting material. With proper adjustment, this process is also economical as it utilizes few supplies. Once grown, the crystals were stored under vacuum.

Only crystals with smooth facets and clean morphologies were used for doping. Those selected were pumped into an argon atmosphere dry box with water and O_2 content nominally less than 2 ppm. The relatively large size of these crystals enables us to adequately control the amount of alkali metal in the system. For example, to dope a 2-mg crystal with potassium (rubidium) metal requires a 1.82- (2.2-) mm length of 0.5-mm-i.d. capillary tube. The metal is measured out by cutting this tube to length inside a glove box equipped with a built-in microscope. For crystals with masses greater than 2 mg, our estimated error in measuring out alkali metal is $\pm 10\%$. After placing the crystal in a 2-mm-i.d. quartz magnetometer tube with the alkali metal, the tube was evacuated to $\sim 10^{-6}$ Torr and sealed.

Doping was carried out in a tube furnace with the crystal at a temperature of 165 °C for potassium doping and 200 °C for rubidium. The dopant was at a higher temperature corresponding to the natural furnace gradient. Once the alkali metal was completely absorbed by the crystal, the sample was annealed for 1–48 h at the same temperature. Rubidium samples generally required much longer anneal times to achieve a maximal superconducting fraction. Because of the irreversible nature of the doping process,[12] obtaining a high-quality sample is a time-consuming process. It should be noted that the C_{60} crystal must be warmed and cooled slowly to prevent the sample from developing cracks that degrade the superconducting transition. This was found to be especially important after the sample has been doped.

All crystals were characterized with measurements of $4\pi M$ vs T, after cooling in near zero field. Data from potassium and rubidium samples are shown in Fig. 2. The greater than 100% diamagnetic response for K_3C_{60} indicates a near fully superconducting sample with shape effects playing a role. While the Rb_3C_{60} curve shows a greater than 100% diamagnetic signal, $4\pi M$ vs H reveals a response that is slightly less than 100% [Fig. 4(b)]. Calculations of the demagnetization factor for K_3C_{60}, assuming a fully superconducting sample, give values ranging from 0.2 to 0.3. These agree with visual assessments of the crystal dimensions. Only samples with transition widths of less than 1 K (10–90 % shielding) and a high volume fraction were used in this study.

While it is possible to extract the sample from the magnetometer without causing visible damage, if it is thermally cycled too often degradation will cause a broadening of the transition width. Hence, once the sample had been characterized, measurements were carried out without removing it from the magnetometer or subjecting it to rapid temperature fluctuations.

EXPERIMENT AND ANALYSIS

Hysteresis curves were taken from 0 to 5 T over a range of temperatures below T_c. In between temperature changes, samples were warmed to 60 K and the magnetic field was quenched and set such that the remnant field was less than 1 Oe. Once the field was stable, the desired temperature was selected and data were taken over 1/2 of a full hysteresis loop. The SQUID range was kept fixed to minimize time relaxation effects which can cause the signal size to change by as much as 25% over the course of 5 h. A 3-cm scan length was used to reduce field inhomogeneities over the length of the measurement. Some typical curves for K_3C_{60} and Rb_3C_{60} are shown in Figs. 3(a) and 3(b). The same curves are shown in Figs. 4(a) and 4(b) at low field. We note that these data show smooth behavior over the entire range of applied fields and temperatures. Furthermore, the symmetry about the x axis, even at high temperatures, indicates negligible background effects which are prevalent in powder samples.[13] Because of sample demagnetization effects, the signal deviates smoothly from linearity as H_{c1} is approached and exceeded, rather than appearing as a sharp cusp. H_{c1} is typically estimated by identifying the field at which the deviation from linearity exceeds a certain percentage. A linear fit to the data below 10 Oe, where the linear correlation coefficient r was better than 0.999, was used to estimate the point where $4\pi M$ departed from the linear by 2%. Because of the arbitrary nature of this selection, the actual value for H_{c1} is prone to some error. However, a consistent choice of

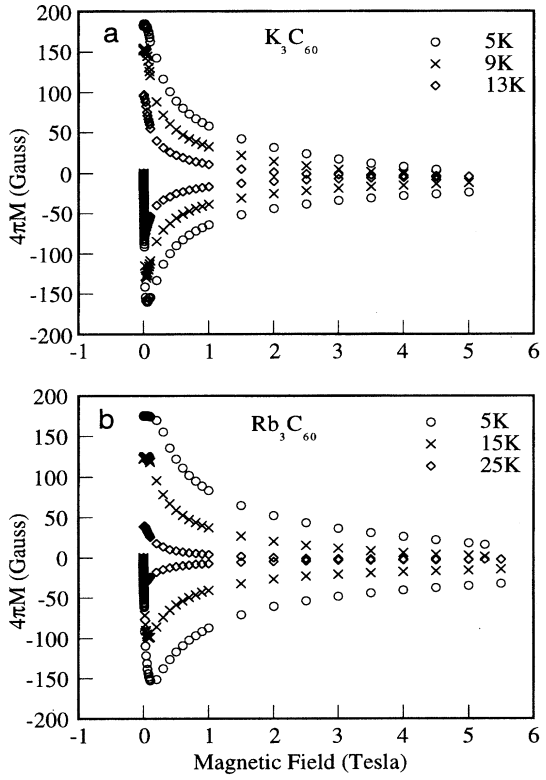

FIG. 3. Half loop hysteresis curves for (a) K_3C_{60} and (b) Rb_3C_{60}.

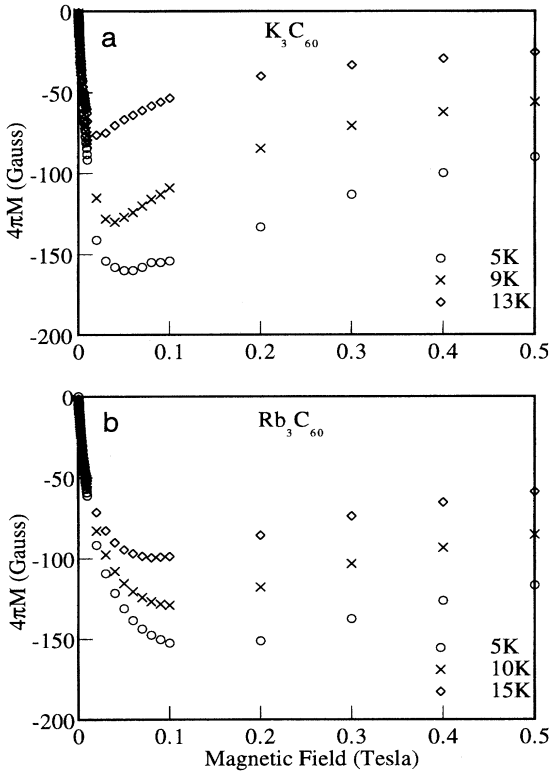

FIG. 4. Low field $4\pi M$ vs H for (a) K_3C_{60} and (b) Rb_3C_{60}.

the deviation should give a reliable dependence on the temperature. In determining values of H_{c1}, we account for the demagnetization factor and the zero offset of the applied magnetic field due to any remnant magnetization in the superconducting magnet.

A graph of H_{c1} as a function of temperature is shown in Fig. 5. Lines are fits to the standard BCS expression

$$H_{c1}(T)=H_{c1}(0)\left[1-\left(\frac{T}{T_c}\right)^2\right]. \quad (1)$$

The data indicate that $H_{c1}(0)$ is 42 ± 1 Oe for K_3C_{60} and 32 ± 1 Oe for Rb_3C_{60}. The difference between these values ($\sim$10 Oe) and the observation that $H_{c1}(0)$ is larger for K_3C_{60} is consistent with other reports obtained by similar methods on polycrystalline samples (Refs. 3 and 4). The fact that $H_{c1}(0)$ is smaller for Rb_3C_{60} points to a larger value for $H_{c2}(0)$ relative to K_3C_{60}, which has been recently reconfirmed.[14,15] In contrast, these past experiments on powders have reported values for $H_{c1}(0)$ that are nearly 3 times larger than those presented here. We should note, however, that measurements of H_{c1} on powders are susceptible to overestimation as a result of surface defects which can pin flux lines as the field begins to penetrate the sample. Single crystals, on the other hand, can suffer from underestimation as a result of demagnetization effects. Our data are in closer agreement with values obtained via muon spin relaxation methods,[16] which is held to be a more direct measurement of the penetration depth λ and hence, the critical field. This research suggests that powders have significant surface defects, the effects of which are magnified by the large total surface area leading to an overestimate of $H_{c1}(0)$. We should add that the curvature in the region of H^*, the point of maximum magnetization, is noticeably smaller for the Rb_3C_{60} sample, which suggests that it possesses a higher degree of inhomogeneity. This observation is consistent with the Rb_3C_{60} phase being more difficult to form due to the 10% size difference between the ions.

For type-II superconductors the critical current J_c can be

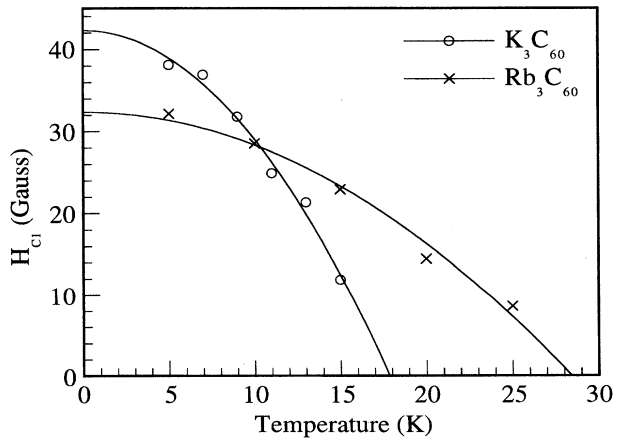

FIG. 5. H_{c1} vs temperature for a 1.54- (2.62-) mg single crystal doped with potassium (rubidium). The lines are fits to Eq. (1).

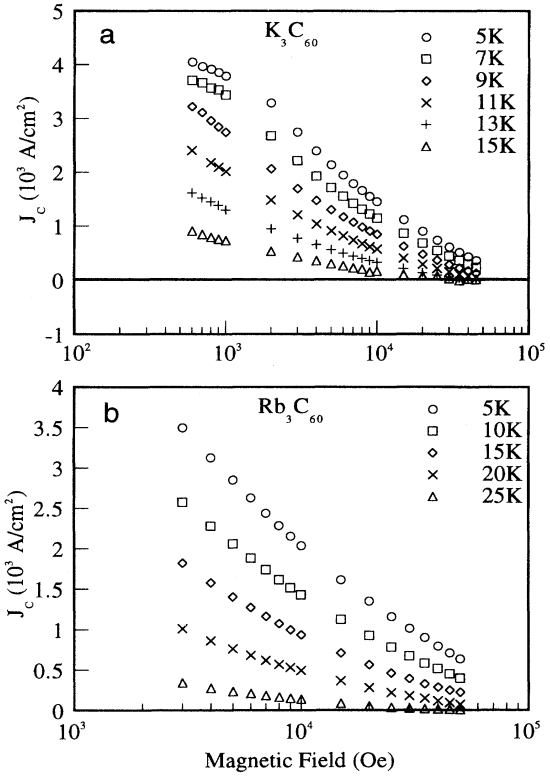

FIG. 6. Logarithmic plot of J_c vs H for (a) K_3C_{60} and (b) Rb_3C_{60} at several temperatures.

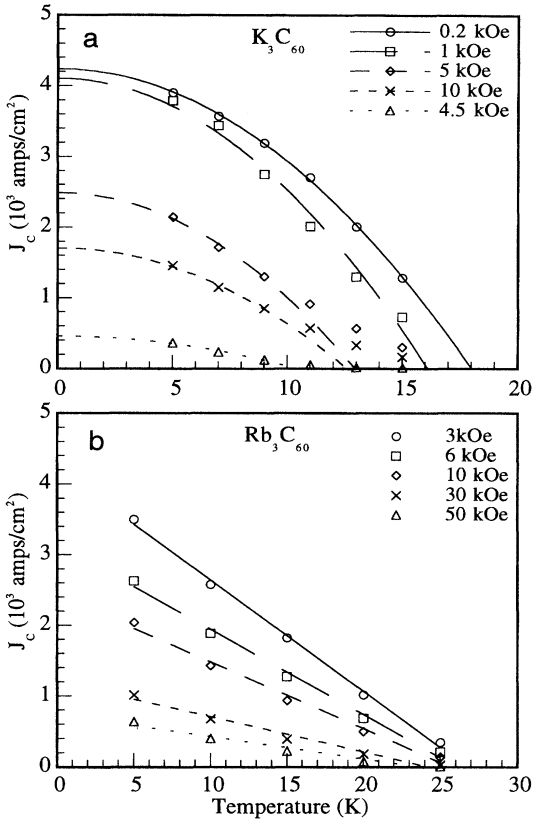

FIG. 7. Critical current density vs temperature at various fields. (a) K_3C_{60}. Lines are fits to Eq. (3). (b) Rb_3C_{60}. Lines are guides to the eye.

estimated by looking at the difference in magnetization of the hysteresis loop for fields between H_{c1} and H_{c2}. The equation provided by the critical-state Bean model[17] has the form

$$J_c(H,T)=\frac{15[\Delta M(H,T)]}{R}, \tag{2}$$

where J_c is measured in units of A/cm^2, $\Delta M(H,T)=(M^+-M^-)$ in emu/cm^3 and R, representing the average grain size of a superconducting particle, in cm. In the case of a fully superconducting single crystal, R reflects the dimensions of the sample. While the model assumes a field-independent J_c, it also requires that the applied fields be much less than H_{c2}. Recent high-field experiments suggest that fields of 1 T are less than 5% of H_{c2} (Refs. 14 and 15). As can be seen in Fig. 6, J_c for our samples is lower by three orders of magnitude than early reports.[3,4,13] However, obtaining an accurate magnitude for J_c is complicated by two factors.

The first comes in estimating R. In the case of powders which can be approximated as a collection of spheres, R is set by the average grain size which can be measured in various ways. With single crystals, certain assumptions must be made about the internal microscopic structure. In the case of the A_3C_{60} (A=K,Rb) single crystals, where the alkali metal is doped in after the raw crystal is grown, it is unlikely that the sample is homogeneous throughout. In fact, it is more probable that the concentration of alkali metal decreases toward the center of the crystal. This implies the existence of nonsuperconducting regions which will place an uncertainty on the determination of an effective R for a crystal specimen of this type. Hence an estimation of R based on the crystal size should be regarded only as a lower bound on the true critical current density.

The second is the sensitive dependence of J_c on the defect structure within the sample. A small J_c suggests there are few defects available for flux pinning,[18] and for single crystals there are likely far fewer surface defects than in powders. Without knowing the relative strengths of these two effects, we should treat the magnitude of J_c as only approximate. However, a great deal of information can still be gleaned by examining the temperature and field dependence of J_c.

Figures 6(a) and 6(b) show a logarithmic plot of J_c vs field for fields above H_{c1}. Each curve represents a different temperature and the basic trend is a decrease of J_c with temperature and field. At higher temperatures and fields the critical current density approaches zero asymptotically. Because of the much broader peak at H^*, data for Rb_3C_{60} are shown only for fields above 2500 Oe. Values of J_c for the potassium- and rubidium-doped samples at low fields and temperatures are quite similar. As the field is increased, however, the magnetization of the rubidium sample retains a larger magnitude and approaches a constant nonzero value as the applied field nears 5 T. This points to stronger pinning forces within the rubidium-doped sample, potentially due to

large scale defects. In both cases, J_c shows a near logarithmic dependence on H and does not correspond to a simple analytic functional form. The smooth character of the data is also different from that derived from powder specimens, which shows a kink in J_c as a function of temperature and is ascribed to the breakdown of intergrain coupling.[19]

For BCS-type superconductors, the temperature dependence has functionally the same form as that of the critical fields:

$$J_c(T)=J_c(0)\left[1-\left(\frac{T}{T_c}\right)^2\right]. \quad (3)$$

Figure 7 shows the temperature dependence of the critical current density at different field strengths. For K_3C_{60} in low fields, the dependence is well characterized by Eq. (3). As the field is increased, however, the curvature decreases and becomes negative. For fields greater than 1000 Oe, the fits exclude points above 10 K for the sake of comparison. This tail is a common phenomenon when measuring the critical fields in high-T_c samples and is attributed to motion of vortices. In the case of Rb_3C_{60} there is little to suggest a dependence of the form of Eq. (3). Given the evidence of a greater number of sample defects, it is possible that they are influencing behavior at lower temperatures.

CONCLUSION

We have synthesized large samples of both K_3C_{60} and Rb_3C_{60} as single crystals and investigated their magnetic properties. Samples were prepared under similar conditions and characterized magnetically. We report extremely sharp T_c's with transition widths of less than 1 K and superconducting fractions significantly higher than those recorded for powder samples. Measurements of the field dependence of the magnetization indicates an $H_{c1}(0)$ of 42 and 32 Oe for potassium- and rubidium-doped C_{60}, respectively. These values are clearly lower than those previously recorded on powders. This suggests a nonintrinsic effect due to the large surface area present in polycrystalline samples.

We have also measured the field and temperature dependence of J_c via the critical-state Bean model. Along with a relatively small value of $J_c(0)$, we find a near logarithmic decrease in the critical current density with applied field and determine that the temperature dependence for K_3C_{60} can be described by a BCS model. Measurements of the rubidium-doped samples do not show such behavior. We surmise that they suffer from a greater incidence of inhomogeneity and defects which lead to the observed anomalous behavior.

The differences observed between the potassium- and rubidium-doped C_{60} samples are likely due in larger part to sample synthesis than intrinsic properties. This is supported by the experimentally well-established property of these compounds that notes that the alkali metal ion plays no role except as an electron donor and to expand the lattice. Hence sample properties for this system should be similar up to a scaling factor. However, when doping large single crystals, it becomes much more difficult to ensure that the samples possess the same degree of homogeneity. As a result, sample defects seem to play a greater role in the rubidium-doped samples. Further investigations, including single-crystal x-ray data and measurements in high field are needed to resolve this question.

The authors would like to acknowledge John Dykes for laying the groundwork for these studies. Research was supported by the National Science Foundation under Grant No. DMR-94-03895 and the Air Force Office of Scientific Research under Contract No. AFOSR-F49620-92-J-0514.

[1] W. Krätschmer, L. D. Lamb, K. Fostiropoulos, and D. R. Huffman, Nature **347**, 354 (1990).
[2] M. J. Rosseinsky *et al.*, Phys. Rev. Lett. **66**, 2830 (1991).
[3] K. Holczer *et al.*, Phys. Rev. B **67**, 271 (1991).
[4] G. Sparn *et al.*, Phys. Rev. Lett. **68**, 1228 (1992).
[5] V. Buntar U. Eckern, and C. Politis, Mod. Phys. Lett. B **6**, 1037 (1992).
[6] J. G. Hou *et al.*, Solid State Commun. **86**, 643 (1993).
[7] J. G. Hou *et al.*, Physica C **228**, 175 (1994).
[8] Quantum Design, San Diego, CA.
[9] T. T. Anderson *et al.*, Rev. Sci. Instrum. **65**, 3820 (1994).
[10] L. Isaacs, A. Wehrsig, and F. Diederich, Helv. Chim. Acta **76**, 1231 (1993).
[11] M. Haluska *et al.*, Appl. Phys. A **56**, 161 (1993).
[12] J. G. Hou, X.-D. Xiang, M. L. Cohen, and A. Zettl, Physica C **232**, 22 (1994).
[13] C. Politis, V. Buntar, W. Krauss, and A. Gurevich, Europhys. Lett. **17**, 175 (1992).
[14] C. E. Johnson *et al.*, Phys. Rev. B **46**, 5880 (1992).
[15] G. S. Boebinger *et al.*, Phys. Rev. B **46**, 5876 (1992).
[16] Y. J Uemura *et al.*, Nature **352**, 605 (1991).
[17] C. P. Bean, Phys. Rev. Lett. **8**, 250 (1962).
[18] A. C. Rose-Innes and E. H. Rhoderick, *Introduction to Superconductivity* (Pergamon, New York, 1978), pp. 202–206.
[19] C. Politis, V. Buntar, and P. Seminozhenko, Int. J. Mod. Phys. B **7**, 2163 (1993).